Ultra High-Resolution FDTD Modeling of a High-Performance VLSI Package for Identifying Resonances and Coupling

César Méndez Ruiz and Jamesina J. Simpson

Electrical and Computer Engineering Department
University of New Mexico, Albuquerque, NM, 87106, USA
cmendezr@unm.edu, simpson@ece.unm.edu

Abstract ─ It is becoming increasingly important to computationally predict, study, and prevent electromagnetic compatibility (EMC) issues arising within and between ICs and other components comprising portable electronic devices. Here, we conduct a phenomenological study involving an ultra high-resolution, three-dimensional finite-difference time-domain (FDTD) model of a sample IC package having over one billion grid cells. Specifically, we determine the resonances and coupling patterns arising within the highly complex IC package. The frequency range of interest extends from 100 MHz to 7 GHz. Results indicate that the arrangement and geometry of the separate power, ground, and signaling networks comprising the IC package greatly influences the electromagnetic behavior within different regions of the package.

Index Terms ─ Digital electronics, EM compatibility, EM coupling, FDTD, resonance, very-large-scale integration.

I. INTRODUCTION

Unintended electromagnetic interference occurring within an integrated circuit (IC) package or via external coupling is a large concern in the design of ICs as well as for the operation of portable electronic devices. ICs are continually being designed to operate at higher clock speeds, be powered with lower supply voltages, and be integrated at higher densities. Further, many modern platforms such as notebooks and ultra mobile devices are continually increasing in functionality while also becoming more compact in size. As a result, ICs must be positioned closer and closer in proximity to other ICs as well as to a variety of high performance wireless communication systems such as Wi-Fi, VoIP, WiMAX, and Bluetooth [1-3], in addition to near field communication technology. All of these trends are causing electromagnetic compatibility (EMC) issues to greatly influence the reliability and operation of electronic devices. As a result, as the technology progresses, EMC must be at the core of the design process of these devices and their components. This is particularly true for ICs, since they tend to be the most susceptible component of the system due to risks of over-voltage or over-current.

Initial EMC research focused on ICs can be traced back to 1965. The effects of EM fields from nuclear explosions on electronic devices were studied at the Special Weapons Center based at Kirtland Air Force Base, Albuquerque, New Mexico, USA. The simulation software SCEPTRE [4] was developed by IBM as a result of this pioneering work. Since this initial research, there have been additional efforts to study the EMC performance of ICs. However, most of the research has been focused on the external region of the packaging. Further, an example analysis of ICs has relied on a complicated integration of measurements, simulations, and analytical calculations through the use of macromodels [5]. In fact, as recently as 2005, the authors of [5] state that for studying ICs, "the combination of propagation effects with possibly very complex geometry… makes a direct full-wave approach not feasible."

More recently, an unconditionally stable time-domain technique using Laguerre polynomials is employed in [6] to develop a methodology for

chip-package cosimulation of ICs. In that work, the IC is divided into sub-blocks (the signal delivery and power delivery networks) for analysis using a full-wave Laguerre equivalent circuit procedure before integrating the results together.

In the present work, we instead take advantage of the computational power afforded by today's supercomputers and simulate on a grand scale a complete IC package as well as the underlying printed circuit board (PCB). Specifically, we solve the full Maxwell's equations using an ultra high-resolution, three-dimensional (3-D) finite-difference time-domain (FDTD) [7, 8] model having over 1 billion grid cells and simultaneously accounting for the power, signal, and ground networks (which we will term functional layers) of the IC package. All of our models are original and do not involve any commercial software.

The simulations and results provided in this paper are directed towards obtaining resonance and coupling patterns throughout the IC package under varying excitation scenarios. Utilizing 384 processors, each of the excitation scenarios for this detailed model takes 26 hours to run. The frequency range of interest extends from 100 MHz to 7 GHz.

This phenomenological study represents a major advance towards enabling engineers to obtain a comprehensive understanding of the fundamental physics behind EMC issues within ICs, and towards providing design parameters necessary for improving and optimizing IC package layouts.

Previously, two related conference abstracts [9, 10] briefly described the general modeling approach employed for this study. A brief description of the sample IC package as well as one example snapshot of electromagnetic energy propagating within one layer of the package was then provided in [11]. This paper, however, significantly builds off of the work of [9-11] by providing a detailed analysis of the electromagnetic behavior, particularly resonances and coupling, within different regions of the IC package and for varying excitations of the IC package. The detailed model descriptions as well as all of the result figures and analyses are original to this paper.

State of the art IC EMC laboratory test techniques are based on measuring either the emissions from the IC (TEM cells, pin current measurements, and near-magnetic field scans) or the susceptibility to electromagnetic noise (bulk current injection, direct power injection, and field coupled) [12]. The common characteristic in all these methods is that the instrumentation is located external to the IC and therefore are not suitable for direct comparisons against the results presented in this paper that concern the inside of the package.

The analysis provided in this paper is unique because the geometry of the layers of the IC package does not behave in an analytically predictable nature. For example, the periodic vias comprising each layer are not all connected to the same adjacent conducting planes (layers); the vias are instead each assigned to one of the three different functional layers (signal, ground, power) and as such many of them must extend through some conducting layers of a different functional type without forming an actual connection. As a result, the vias within the different regions of the package do not behave in a manner according to typical electromagnetic bandgap structures or substrate integrated waveguides as in [13].

The remainder of this paper is organized as follows. Section II below demonstrates the validity of the code by duplicating results of similar structures reported by other authors. Section III below provides an overview of the FDTD model. Section IV describes the general methodology of the analysis and the simulation cases that are considered. The corresponding simulation results are then documented and discussed in Section V. Finally, section VI concludes the paper.

II. CODE VALIDATION

In order to validate the code that is used for the modeling of the IC package we first successfully reproduce results obtained for a similar, but much simpler structure as reported by Shahparnia et al. [14, 15]. In these references, the authors developed an analytical model to predict the resonant properties, pass-band, and stop-band of electromagnetic bandgap (EBG) structures embedded in PCBs and packages. They compare their results against finite element (FE) based results. The frequency range of interest, gap between conducting planes and via diameter are comparable to those corresponding to the IC package analyzed in this paper. A lateral view of the considered 3-D structure is shown in Fig 1.

Table 1: Comparison of FDTD model calculations and results reported in [14]

d (mm)	a (mm)	h_1 (mm)	h_2 (mm)	ε_{r1}	ε_{r2}	*Vias diameter* (μm)	FE Gap (GHz)	Model Gap (GHz)	FDTD Gap (GHz)
10.4	10×10	1.54	1.54	4.1	4.1	800	2.1-4.0	2.5-4.0	2.0-3.9
10.4	10×10	1.54	1.54	8.2	4.1	800	1.6-3.7	1.8-3.7	1.7-4.0
10.4	10×10	1.54	1.54	12.3	4.1	800	1.3-3.1	1.5-3.5	1.4-3.6
10.4	10×10	1.54	1.54	16.4	4.1	800	1.2-2.9	1.3-3.4	1.3-3.3
2.2	2×2	0.016	0.1	4.1	4.1	125	6.0-18.1	6.1-14.7	7.2-19.5

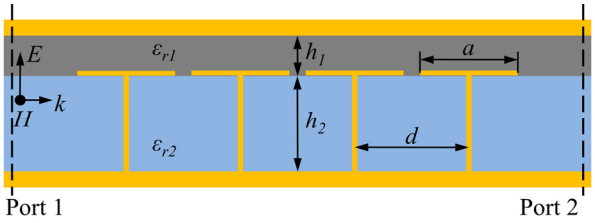

Fig. 1. EBG structure embedded in a PCB. Four infinitely long rows of EBG cells are placed between the 2 ports that are used to calculate the S parameters.

Table 1 collects the band-stop frequency range of various EBG structures. The limits of the gap are determined by a -20 dB criteria of the scattering parameter S_{21}. For all considered cases, the FDTD model shows satisfactory agreement, in particular with the results obtained from the FE simulations.

III. FDTD MODEL OF SAMPLE IC PACKAGE AND PCB

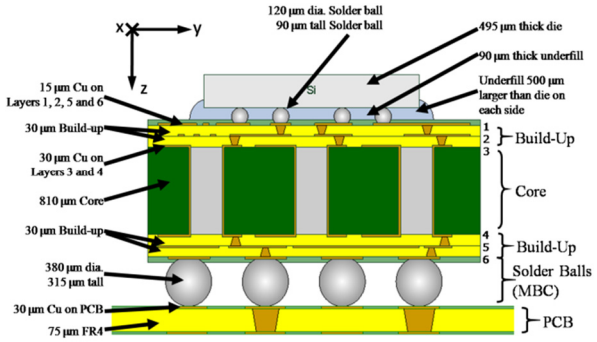

Fig. 2. General cross-sectional view of the sample six-layer IC package with the underlying sample PCB.

The FDTD model employed in this study encompasses 2580×2580×160 grid cells in each x, y, and z Cartesian direction to finely model the sample IC package and the underlying sample PCB. A general schematic of the model is shown in Fig. 2. The complete FDTD model includes details of the conducting layers, silicon, dielectrics, vias, ground / power traces, and solder balls. For a practical implementation of such demanding computation and storage it becomes necessary to exploit the parallel processing techniques. Specifically, we employ the domain decomposition parallelism scheme in which the computation domain is divided into equal rectangular sub-areas. The essential elements of a parallel algorithm for the FDTD method using the message passing interface (MPI) library are reported in [16].

Figures 3, 5, and 6 are designed with a specific color code to identify materials and functional layers. The white color was defined to represent air, red corresponds to any dielectric, yellow corresponds to ground, green corresponds to power and blue corresponds to signal.

There are in total six conducting layers in the IC package. Conducting layers 2, 4, and 6 are ground planes while conducting layers 3 and 5 belong to the power network. Conducting layer 1 is split into two conducting surfaces of equal area as shown in Fig. 3: the left side is ground and the right is power. The via pitch under the die shadow is denser than outside the die shadow (320 μm vs. 1 mm). The PCB is comprised of two conducting planes; one is power and the other is ground.

Each via within the structure is assigned to the signal, ground, or power function layer. Each via is thus only connected to its corresponding signal / ground / power conducting layer, respectively. That is, the ground and power vias are shorted at each end only to ground and power conducting layers, respectively, and the signal vias are connected to ground conducting layers through lumped resistors. As a result, because the ground, signal, and power conducting layers alternate through the structure, the vias must extend through an opening through some conducting planes to connect to a conducting plane further away. This geometry greatly complicates the electromagnetic behavior throughout the entire IC package.

The FDTD grid has a uniform cell size of 10×10×15 μm in x, y, and z-directions, respectively. This resolution is high enough to resolve the smallest circular via diameter within the model without introducing stair-casing effects into the computational results.

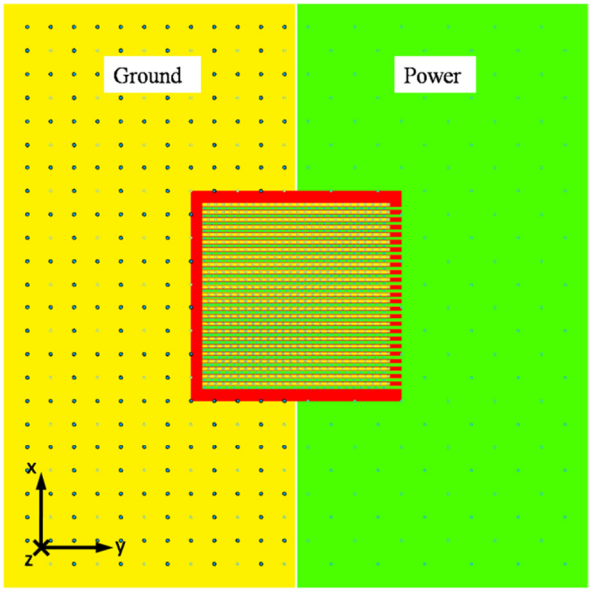

Fig. 3. Detailed top view of the IC package conducting layer 1 of Fig. 1. The circles represent the via/via pad/via anti-pad locations.

Table 2 lists all materials within the model and their corresponding electrical properties. The conductivities are calculated assuming a clock frequency of 1 GHz.

Table 2: Materials properties

Material	Relative Permittivity (ε_r)	Loss Tan	Conductivity (S/m)
Silicon	10.24	0.025	0.01420
Underfill	3.5	0.025	0.00487
Build-Up	3.7	0.017	0.00350
Core	4.6	0.017	0.00435
FR4	4.3	0.017	0.00407

IV. METHODOLOGY AND SIMULATION CASES

A total of six simulation cases are conducted to characterize the resonances and coupling within the package. In all cases, the source is a modulated Gaussian pulse centered at 8 GHz and having spectral energy from 100 MHz to 20 GHz. We primarily consider the frequency range of 100 MHz to 7 GHz, but in a few cases we examine the performance of the IC up to 20 GHz for additional behavioral information.

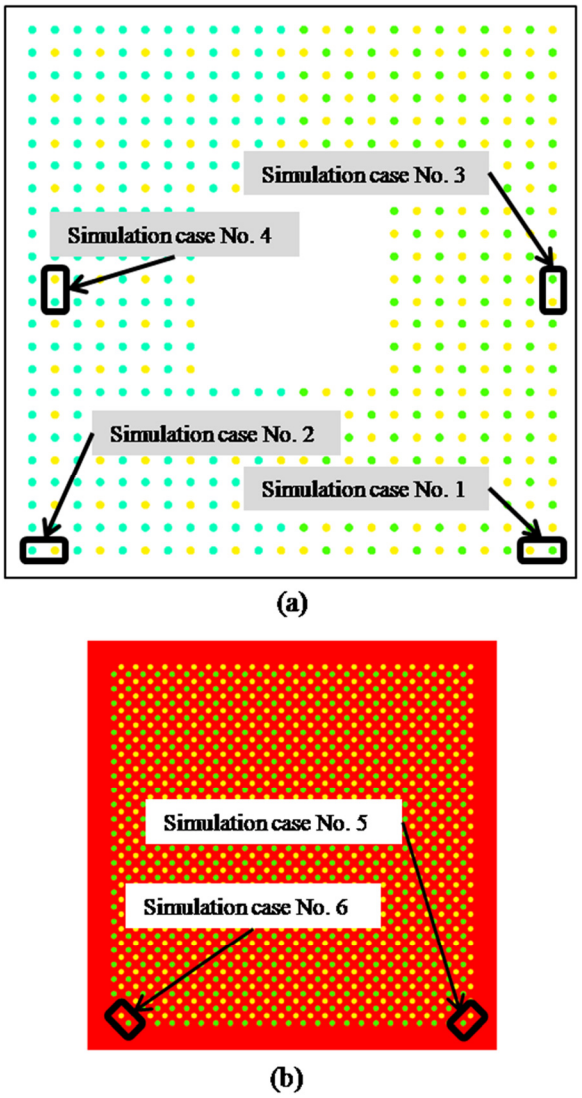

Fig. 4. Sources locations for the different simulation cases. (a) Motherboard connection solder balls. (b) Solder balls in the under-fill region, a zoomed-in view to the under-die zone.

For each simulation case, two neighboring solder balls are excited with the source waveform skewed at 50%. The excitation is implemented as a set of lumped resistive voltage sources [17] along the surface of both solder balls so that the total resistance of each lumped resistive source is 50 ohms. The unique feature of each simulation case is the location of these sourced pair of solder balls. Figure 4(a) shows the source locations for simulation cases 1 – 4 having the excitation implemented at two motherboard connection

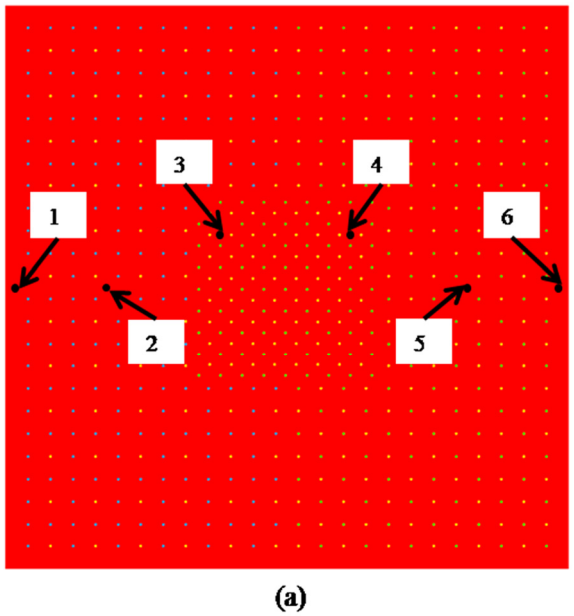

Fig. 5. Locations and numbering of each observation point at which the electric fields are recorded. (a) Build-up between conducting layers 4 and 5. (b) Build-up between conducting layers 1 and 2.

solder balls between conducting layer 6 and the PCB upper conducting layer. Likewise, Fig. 4(b) shows the source locations for simulation cases 5 and 6 having the excited solder balls in the underfill region connecting the die with the packaging. Each of the two exited solder balls belongs to a different functional layer. For example, for Simulation Case 1, a solder ball at

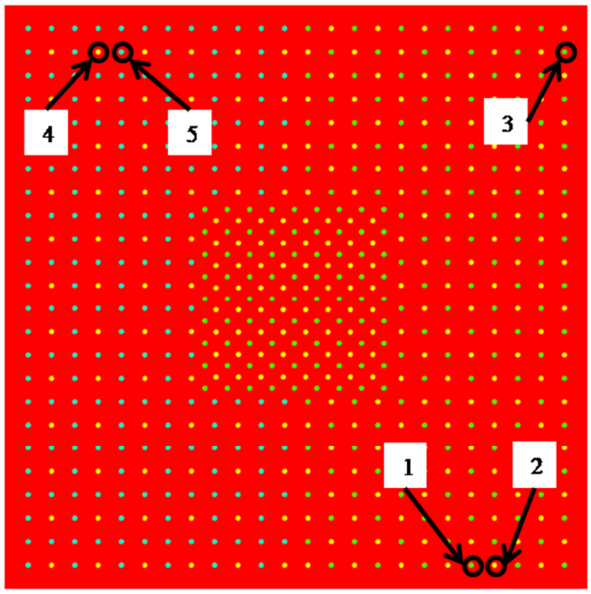

Fig. 6. Location and numbering of the vias between Layers 3 and 4 at which the electric conduction currents are computed.

the lower right corner of the package belonging to the power network is excited, along with a neighboring solder ball to its left belonging to the ground network. Similarly, in Simulation Cases 3, 5, and 6, two neighboring power and ground solder balls are excited as shown in Fig. 4. And in Simulation Cases 4 and 2, two neighboring signal and ground solder balls are excited.

The response of the package to the excitations is based on analyzing the behavior of the electric field throughout the IC, as well as the electric conduction current flowing through the vias. Specifically, the z component of the electric field (Ez) is recorded versus time during each of the six simulation cases at 64 observations points. Figure 5 shows eight key observation points that will be used in this paper to illustrate the variation of the resonances within different zones of the package.

To compute the electric current (Iz), an Ampere's Law contour-line integration of the magnetic field is performed around the vias, of which we have selected five (from 90) to best illustrate the results. Each integration path for these five selected vias lies in the x-y plane at the midpoint between Conducting Layers 3 and 4 as shown in Fig. 6.

The data for both Ez and Iz are normalized relative to the source spectral waveform and then to the maximum value of the response at the

observation point or via having the strongest response to the excitation obtained during time stepping for each corresponding simulation. This second normalization step allows us to compare relative to each other the magnitudes of the observed values within each separate simulation case.

The normalization procedure may be expressed as

$$a_i(f) = \frac{\frac{A_i(f)}{S(f)}}{MAX\left[\frac{A_{reff}(f)}{S(f)}\right]}, \quad (1)$$

where a_i and A_i refer, respectively, to the normalized and un-normalized values of E_z or I_z for the observation point or via i as a function of frequency f. S refers to the source waveform. The reference A_{reff} is taken to be the corresponding E_z or I_z having maximum peak response to the excitation source relative to the other studied locations for that particular simulation case.

V. RESULTS AND ANALYSIS

The computational results demonstrate that the frequency content of the EM energy observed propagating through the package is determined to be dependent on the spatial location of the source and observation point within the structure and relative to each other. The complex sample package of Fig. 2 therefore cannot be analyzed using the results of a single simulation. Some regions of the package block certain ranges of spectral energy, while the conducting layers naturally block all of the electromagnetic energy within the frequency range of interest. Additionally, mutual coupling shifts the spectral energy and resonances throughout the structure. As a result, different simulation scenarios are performed with the sources spatially varied for each case in order to characterize which zones of the structure lead to specific resonances and behaviors. In this Section, we utilize the results from six simulation cases to demonstrate the resonances, coupling, and shielding produced by different zones within the package.

A. Electric conduction currents

As stated earlier, the package is comprised of a ground network, power network, and signaling vias (functional layers). The computed currents at different vias corresponding to these different functional layers indicate that each functional layer has its own set of resonant frequencies. Because of mutual coupling, these resonances continually shift towards or away from each other as the observation position moves within the package. Simultaneously, we observe in some regions of the structure that some spectral energy is shifted even to spectral ranges not included in the source spectrum (well above 20 GHz). Only while the EM energy propagates through a uniform dielectric region of dimensions on the order of a wavelength do the resulting resonant frequencies remain constant with position.

Simulation Case 1 best illustrates the shifting of the resonances due to mutual coupling. The electric current at Via 1, which is positioned almost directly above the sourced solder balls, shows that the power network resonates at 1.42 and 6.74 GHz. Similarly, the current at Via 2, also positioned almost directly above the sourced solder balls, shows that the ground network resonates at 2.66 GHz. Both Via 1 and Via 2 currents are illustrated in Fig. 7. As we move laterally away from the source location, however, any other vias within the power or ground networks on the right side of the package are found to have resonant frequencies between those of Vias 1 and 2. This is illustrated in Fig. 8 for Via 3, which is on the same right side but opposite end of the structure relative to the sourced solder balls. Via 3 has two resonant frequencies: one at 1.58 which is between the 1.42 and 2.66 GHz resonant frequencies of Vias 1 and 2 and the other at 4.38 GHz which is between the 2.66 and 6.74 GHz resonant frequencies of Vias 1 and 2. Further observations indicate that the higher 4.38 GHz resonance of Via 3 diminishes rapidly as the EM energy propagates through the outer periodic ground and power vias on the right side of the package positioned outside the shadow region of the die. However, the resonance at 1.58 GHz can propagate through these periodic vias.

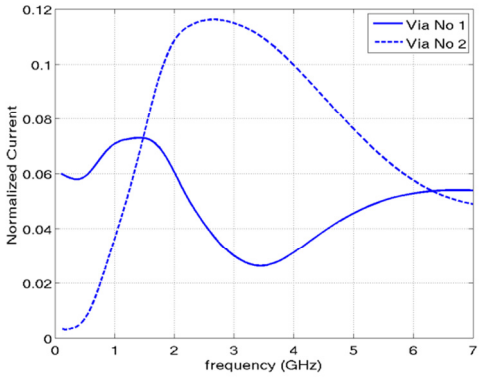

Fig. 7. Spectral response of the electric current at Vias 1 and 2 for Simulation Case 1.

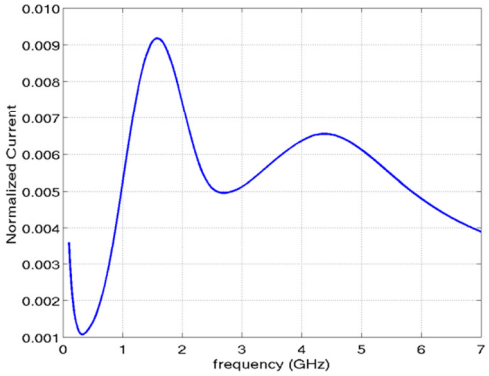

Fig. 8. Spectral response of the electric current at Via 3 for Simulation Case 1.

Regarding the left side of the package, we find from Simulation Case 2 that the ground network weakly resonates at 0.88 GHz on the left side of the package (same side as the sourced solder balls) within the main frequency range of interest (100 MHz to 7 GHz). Figure 9 shows this resonance for Via 4 (ground via), which is positioned on the same left side but opposite end of the structure relative to the sourced solder balls. However, by checking the spectral data of this same via current up to 20 GHz (shown in Fig. 10) instead of 7 GHz, it can be seen that most of the resonance spectral energy of the ground network is above our main frequency range of interest. Within the range of 100 MHz to 7 GHz, the magnitude of the current flowing through each of the signal vias is always an order of magnitude lower than the current flowing through any of its neighboring ground vias. These signal vias thus act to block the EM energy on the left side of the package.

We also find from Simulation Case 2 that the signal vias on the left side of the package do not have any defined resonances between 100 MHz and 7 GHz. Further, most of the signal vias currents on the left side of the package are above 10 GHz, as illustrated for Via 5 (signal via) in Fig. 10.

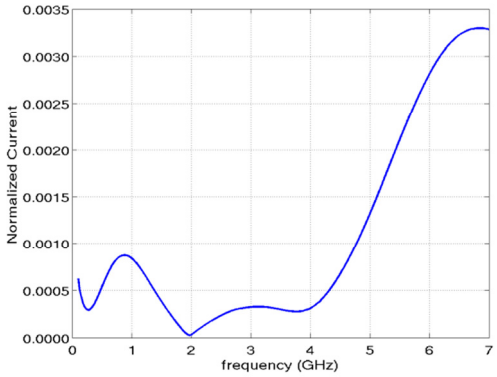

Fig. 9. Spectral response of the electric current at Via 4 for Simulation Case 2.

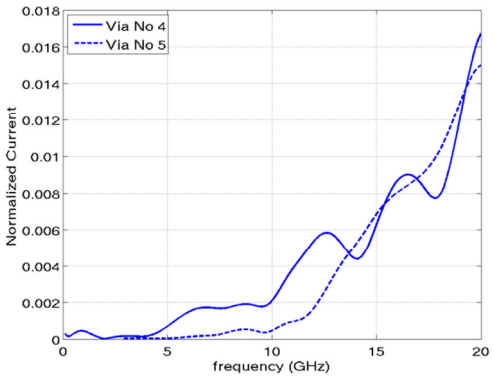

Fig. 10. Spectral response up to 20 GHz of the electric current at Vias 4 and 5 for Simulation Case 2.

B. Electric fields

The build-up between conducting layers 4-5 and 5-6 has two main resonant frequencies on the right side of the package. This is illustrated in Fig. 11 for Simulation Case 1. At observation point 6 (located between conducting layers 4-5 on the same right side of the structure as the sourced solder balls), Ez is observed to have resonances at ~1.80 GHz and ~5.34 GHz, with the higher frequency (~5.34 GHz) resonance being wider band. Note that for Via 3 the Iz resonances were found centered at 1.58 and 4.38 GHz. This further

illustrates the continual shift of resonant frequencies with position. Further, by comparing observation point 6 (positioned on the periphery of the package, just outside the periodic vias) of Fig. 11 with observation point 5 (positioned almost half-way towards the center of the structure) of Fig. 12, it is observed that the higher frequency 5.34 GHz resonance diminishes as the energy propagates from the periphery of the packaging into the periodic structure formed by the vias.

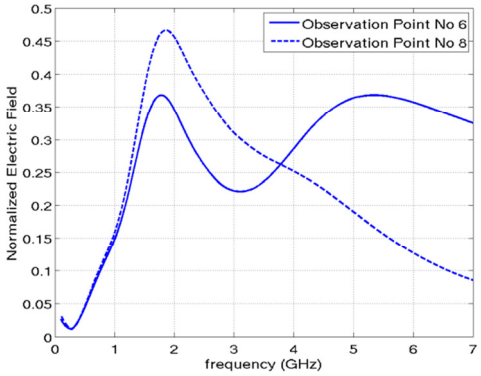

Fig. 11. Spectral response of the electric field at observation points 6 and 8 for Simulation Case 1.

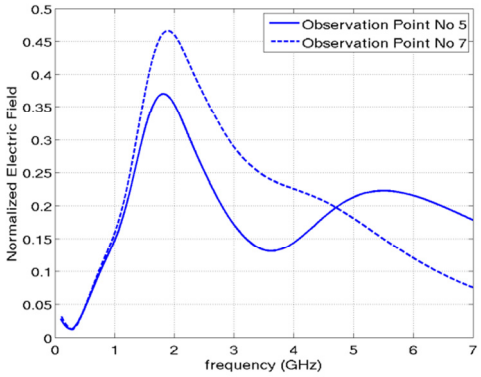

Fig. 12. Spectral response of the electric field at observation points 5 and 7 for Simulation Case 1.

The lower frequency (~1.80 GHz) resonance on the right side of the package is found to be stronger within the build-up between conducting layers 1-2 and 2-3 than in the build-up between conducting layers 4-5 and 5-6. Observation points 7 and 8 (shown in Figs. 11 and 10, respectively) demonstrate these using results from Simulation Case 1. Additionally, the higher frequency resonance (at ~5.34) is no longer present at observation points 7 and 8.

Figure 13 is an example 2-D slice of Ez values that demonstrates the resonances occurring within the core for Simulation Case 1. It is observed that the periphery of the package acts like a transmission line wherein the EM energy propagates at the higher frequencies (5.34 GHz). The reduction of this ~5.34 GHz energy as the EM energy propagates into the periodic vias is also observable in Fig. 13.

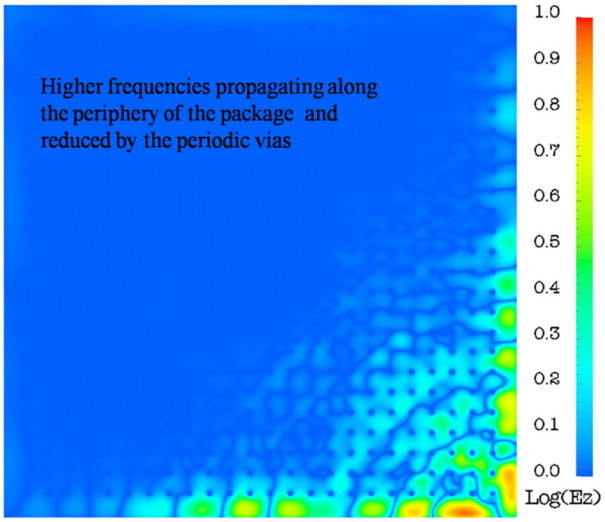

Fig. 13. Electromagnetic energy propagating through the core for Simulation Case 1. A planar cut of Ez values at the midpoint of the gap between conducting layers 3 and 4 is shown.

Simulation Cases 5 and 6 show that the region below the die has two resonances, one at ~500 MHz and the other at ~1.6 GHz (shown in Fig. 14). The strongest amplitudes at these frequencies are located in the build-up between conducting layers 4-5 and 5-6, however these resonances are also significant in the solder balls connecting the silicon layer to the package (underfill layer) as well as in the build-up between conducting layers 1-2 and 2-3. Interestingly, for different Simulation Cases, and thus source locations, these two resonances are also shifted towards each other by varying amounts, resulting for Simulation Cases 1 and 3 in a single but wider bandwidth resonance.

In all of the simulation cases, the strongest response always lies in the build-up layers between conducting layers 1-2, 2-3, 4-5 and 5-6 (numbered according to Fig. 2), but not in the core (between conducting planes 3-4).

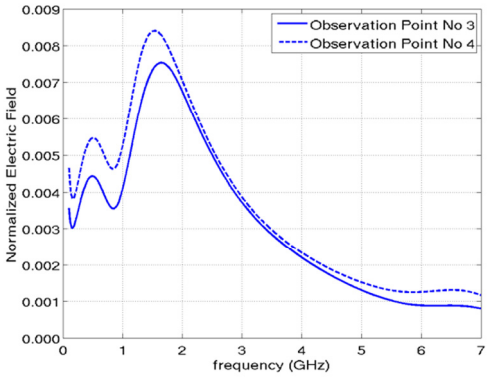

Fig. 14. Spectral response of the electric field at observation points 3 and 4 for Simulation Cases 5 and 6, respectively.

This is because no vias are terminated in conducting layers 3 and 4 bounding the core. That is, at every connection of a via to a conducting plane, EM energy is radiated, and since no vias are terminated on either side of the core, the signal energy is lower within that region. For example, in the snap-shot of Ez shown in Fig. 15, the 1st and 3rd vias (from right to left) are terminated in conducting layer 1. As a result, these vias radiate energy outside (above) the package as well as in the build-up between conducting layers 1 and 2. The 2nd via, however, is terminated in conducting layer 2 and as a result does not radiate energy above the package (above conducting layer 1), but instead radiates energy upwards between conducting layers 1 and 2, and downwards, between conducting layers 2 and 3.

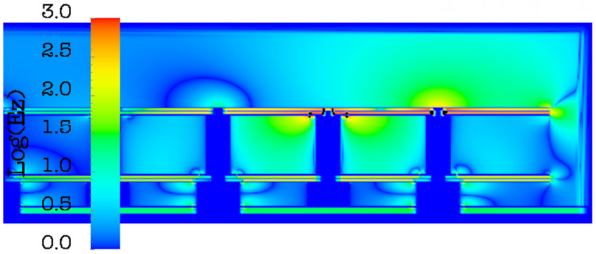

Fig. 15. EM energy propagating through the package for Simulation Case 1. Vertical slice of Ez intersecting the center of Vias 1 and 2. Zoomed-in view to the three right most vias of the entire structure.

Regarding the left side of the package, only the build-up between conducting layers 4-5 and 5-6 resonate weakly at ~680 MHz, as observed at observation point 2 for Simulation Case 2. But as for the analysis of the currents, this resonance can be neglected compared to all the spectral energy present at frequencies above 7 GHz as shown in Fig. 16.

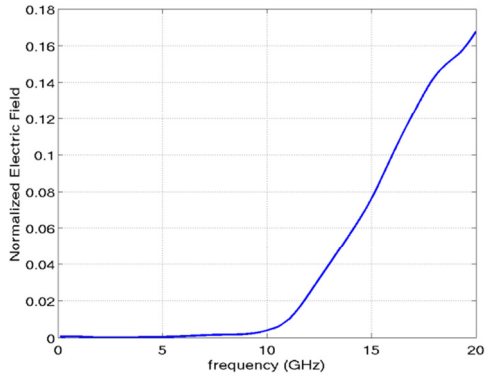

Fig. 16. Spectral response up to 20 GHz for the electric field at observation point 2 for Simulation Case 2.

In Simulation Case 6, which is the only simulation case of the six wherein the source is located on the left side of the package and the excited solder balls correspond to the ground and power networks, most of the signal energy propagates only along the periphery of the left side of the package. This is apparent by comparing observation point 2 with its symmetry observation point 5. A comparison of observation points 1 and 2 for Simulation Case 6 illustrates this effect in Fig. 17.

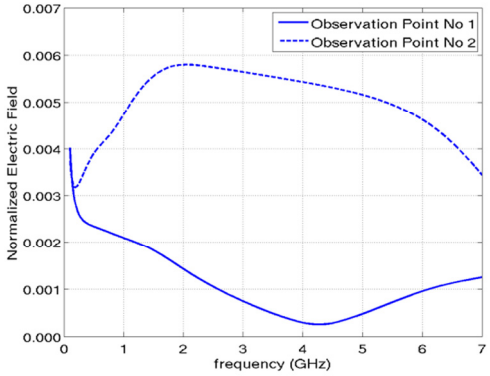

Fig. 17. Spectral response of the electric field at observation points 1 and 2 for Simulation Case 6.

VI. CONCLUSION

We have performed a phenomenological study with the goal of examining resonances and coupling within a sample IC package using a

greater than one-billion cell full-Maxwell's equations FDTD model. Results from six separate simulation cases permitted us to demonstrate the behavior and characteristics of each of the three functional layers of the IC as well as the different regions of the package, such as under-die, left side, right side, core, build-up layers, etc.

Due to the highly complex geometry and interconnections of the IC package along with the effects introduced by the underlying PCB, EMC for IC design is a difficult problem. It is apparent from the results presented in this paper, however, that an external wireless transmitter emitting radiation within the frequency range of 500 MHz to 2 GHz could, depending upon its location and frequency content, present a hazard for specific regions within the IC package. That is, especially if the transmitter's frequency content includes a resonance found in a region of the package and that region of the package lies within a direct propagation path of the transmitter, the radiation from the transmitter may couple into the IC.

ACKNOWLEDGMENT

CONACYT Fellowship number 304287 is partially supporting author C. Méndez Ruiz's (209576) graduate studies.

The authors acknowledge the technical contributions of Bryce Horine and Kevin Slattery of Intel Corporation in defining the realistic sample IC package model used in the analysis of this paper.

Supercomputing resources were provided by the New Mexico Computing Applications Center and by the University of New Mexico's High Performance Computing Center under grant # 2007004.

REFERENCES

[1] "Beyond the Call- Intel and Motorola Explore New Possibilities for the Cell Phone Platform," URL: http://techresearch.intel.com/articles/Exploratory/1431.htm

[2] "Intel's Portable Prototypes," PC Magazine, URL: http://www.pcmag.com/article2/0.2704.1884623,00.aspR. F. Harrington, *Time-Harmonic Electromagnetic Fields*, McGraw-Hill, New York, 1961.

[3] "New Intel Portable PC concept at Computex Paipei 2007," Coolestgadgets.com, URL: http://www.coolest-gadgets.com/20070606/new-intel-portable-pc-concept-atcomputex-taipei-2007

[4] S. R. Sedore, Automated Digital Computer Program for Determining Responses of Electronic Circuits to Transient Nuclear Radiation (SCEPTRE), AFWL TR 66-126, *Air Force Weapons Laboratory*, 1967a.

[5] F. Canavero, S. Grivet-Talocia, I. A. Maio, and I. S. Stievano, "Linear and Nonlinear Macromodels for System-Level Signal Integrity and EMC Assessment," *IEICE Trans. Commun.: Invited Paper, Special section of 2004 International Symposium on EMC*, vol. E88-B, no. 8, pp. 3121-3126, Aug. 2005.

[6] K. Srinivasan, "Multiscale EM and Circuit Simulation using the Laguerre-FDTD Scheme for Package-Aware Integrated-Circuit Design," Ph.D. dissertation, School of ECE, Georgia Institute of Technology, Atlanta, GA, 2008.

[7] K. S. Yee, "Numerical Solution of Initial Boundary Value Problems Involving Maxwell's Equations in Isotropic Media," *IEEE Trans. Antennas Propagat*., vol. AP-14, issue 8, pp. 302-307, May 1966.

[8] A. Taflove and S. C. Hagness, Computational Electrodynamics: The Finite-Difference Time-Domain Method, 3rd edition. Norwood, MA: Artech House, 2005.

[9] J. J. Simpson, B. Horine, and H. Heck, "Ultra High-Resolution FDTD Modeling of an Integrated Circuit Package for Characterizing and Solving EMC Problems in Compact Portable Electronic Devices," *Proc. IEEE AP-S Intern't Symp. and USNC/URSI Nat '1 Radio Science Meeting*, San Diego, CA, July 2008.

[10] J. J. Simpson, "FDTD Full-Maxwell's Equations Modeling from Near-DC to Light," *Proc. 24th Int'l Review of Progress in Applied Computational Electromagnetics (ACES)*, Niagara Falls, Canada, April 2008.

[11] C. M. Ruiz, J. J. Simpson, B. Horine, and K. Slattery, "Utra High-Resolution FDTD Modeling of a High-Performance VLSI Package," *IEEE AP-S International Symposium and USNC/URSI National Radio Science Meeting*, Charleston, SC, June 2009.

[12] S. Ben Dia, M. Ramdani, and E. Sicard, editors, Electromagnetic Compatibility of Integrated Circuits – Techniques for Low Emission and Susceptibility, Springer, 2006.
[13] F. Xu and K. Wu, "Guided-Wave and Leakage Characteristics of Substrate Integrated Waveguide," *IEEE Trans. Microw. Theory Tech.*, vol. 53, no. 1, pp. 66–73, Jan. 2005.
[14] S. Shahparnia and O. M. Ramahi, "A Simple and Effective Model for Electromagnetic Bandgap Structures Embedded in Printed Circuit Boards," *IEEE Microw. Wireless Compon. Lett.*, vol. 15, no. 10, pp. 621–623, Oct. 2005.
[15] S. Shahparnia and O. M. Ramahi, "Miniaturazed Electromagnetic Bandgap Structures for Ultra-Wide Band Switching Noise Mitigation in High-Speedprinted Circuit Boards and Packages," *in Proc. 13th Topical Meeting Electrical Performance Electronic Packaging.*, pp. 211-214, Portland, OR, Oct. 25-27, 2004.
[16] C. Guiffaut and K. Mahdjoubi, "A Parallel FDTD Algorithm Using the MPI Library," *IEEE Antennas Propag. Mag.*, vol. 43, no. 2, pp. 94–103, Apr. 2001.
[17] M. Piket-May, A. Taflove, and J. Baron, "FD-TD Modeling of Digital Signal Propagation in 3-D Circuits with Passive and Active Loads," *IEEE Trans. Microwave Theory and Tech*., vol. 42, no. 8, pp. 1514-1523, Aug, 1994.

César Méndez Ruiz was born in México City, México, on June 1, 1980. He received the B.S. diploma in Electromechanical Engineering from the Universidad Panamericana, Zapopan, Jalisco, México, in 2003, and the M.S. degree in Electronic Engineering from the Universidad de Guadalajara, Guadalajara, Jalisco, México, in 2007. He is currently working toward the Ph.D. degree in Applied Electromagnetics at the University of New Mexico, Albuquerque, NM.
From 2002 to 2003, he was a trainee in Hewlett-Packard (HP). He has professional experience in R&D area working as a mechanical design engineer for HP and Best in Development and Technology (BDT).

Jamesina J. Simpson received the B.S. and Ph.D. degrees in Electrical Engineering from Northwestern University, Evanston, IL, in 2003 and 2007, respectively. As a graduate student, Dr. Simpson was a recipient of the National Science Foundation Graduate Research Fellowship, IEEE AP-S Graduate Research Award, and IEEE MTT-S Graduate Fellowship.
In 2007, Dr. Simpson joined the Electrical and Computer Engineering Department at the University of New Mexico – Albuquerque as a tenure-track Assistant Professor. Her research lab encompasses the application of the full-Maxwell's equations finite-difference time-domain (FDTD) method to model a wide variety of scientific and engineering applications. In 2010, Dr. Simpson was awarded an NSF CAREER grant.